# A characterization technique for quantum well infrared photodetectors

C. J. Chen, K. K. Choi,[a),b)] L. Rokhinson, W. H. Chang,[b)] and D. C. Tsui

*Department of Electrical Engineering, Princeton University, Princeton, New Jersey 08544*

Despite the rapid development of the quantum well (QW) infrared technology, the intrinsic properties of the QW infrared photodetectors (QWIPs) have not been directly measured under the operating conditions of the detector. In this work, we introduce a characterization technique, which utilizes the surface corrugation to probe the absorption coefficient and the photoconductive gain of a QWIP under different operating conditions. This technique enables the intrinsic properties of the detector to be more accurately characterized and its performance better assessed. A mid-wavelength QWIP is used for the demonstration of this technique. The results are compared to those deduced from the conventional measurements. © *1999 American Institute of Physics.*
[S0003-6951(99)02246-9]

Quantum well (QW) infrared photodetectors (QWIPs) have many military and civilian applications.[1,2] The recent employment of the corrugated light coupling scheme[3] further improves the detector sensitivity, manufacturability, and functionality (such as remote temperature sensing[4] and polarization-sensitive detection[5]). However, despite the rapid developments of the QWIP technology, some important parameters of the detector, such as the absorption coefficient $\alpha$ and the photoconductive gain $g$, still cannot be accurately measured under the operating conditions of the detector. In this work, we propose to use the surface corrugation in the corrugated-QWIP (C-QWIP) structure as a probing tool to measure $\alpha$ and $g$ directly. This technique can be applied to different material structures and operating conditions, and thus is capable of providing more detailed and relevant information on the intrinsic properties of the QWIPs. With this information, the detector performance can be further improved.

To characterize the optical properties of a QWIP, one usually measures the responsivity $R$, which is expressed as

$$R = \frac{e}{h\nu} \cdot \eta g, \tag{1}$$

where $h\nu$ is the incident photon energy and $\eta$ is the quantum efficiency under a specific light-coupling scheme. If one of the two parameters, $\eta$ or $g$, can be measured accurately, the other can then be determined using Eq. (1). However, there are difficulties in measuring either of these two parameters. For example, Fourier transform infrared spectroscopy (FTIR) is usually used to measure the infrared absorption $\alpha$ at a particular oblique angle. The value of $\alpha$ for parallel propagating light, on which $\eta$ of an efficient light coupling scheme depends, cannot be directly measured. Furthermore, for QWIP samples with weak intersubband transitions, accurate absorption measurement can be difficult. Similarly, problems exist in using the conventional approach of the noise measurement to determine the $g$ value. In this approach, an assumption is made that the photoconductive gain $g$ and the

noise gain $g_n$ are equal. In reality, however, $g$ varies with the energy of the charge carriers, while $g_n$ obtained from the noise measurement depends only on the average energy. Under various operating conditions, the energy distribution of the charge carriers could be different. A technique capable of resolving the energy spectrum of $g$ is therefore needed to properly characterize the detector performance.

We have developed a technique that allows direct measurements of the absorption coefficient $\alpha$ and the photoconductive gain $g$ at any incident wavelengths under different operating conditions. In this approach, an array of V grooves is chemically etched into the active volume of a QWIP to form the C-QWIP structure. A set of C-QWIPs with different V-groove periods is prepared. The side view of a C-QWIP having four corrugation units is illustrated in Fig. 1. The 50° inclined sidewalls are utilized to reflect the normal incident light into a parallel direction to the QW layers so that the $s$ polarization of the incident radiation can be absorbed. As a result, the intensity of the $s$ polarization decays exponentially as light propagates away from the sidewalls. Since the detector substrates are partially thinned, the measured absorption also includes any possible waveguiding effects of the substrate on the optical path. Assuming negligible light interference effect inside the detector, the responsivity of the C-QWIP with period $P$ is given by

$$R(P) = \frac{e}{h\nu} \cdot g \, \eta(P)$$

$$= \frac{e}{h\nu} \cdot g \cdot \frac{\alpha}{2P} \cdot \int_0^t \int_0^{P-2z} \left[ e^{-\alpha \cdot x} + e^{-\alpha \cdot (P-2 \cdot z - x)} \right]$$

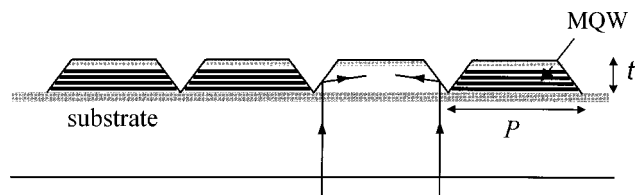$$\times dx \; dz + R_0, \tag{2}$$



FIG. 1. The profile of a C-QWIP with etching depth $t$ and corrugation period $P$. The sidewall angle is 50°.

[a)]Electronic mail: kchoi@mail.arl.mil.
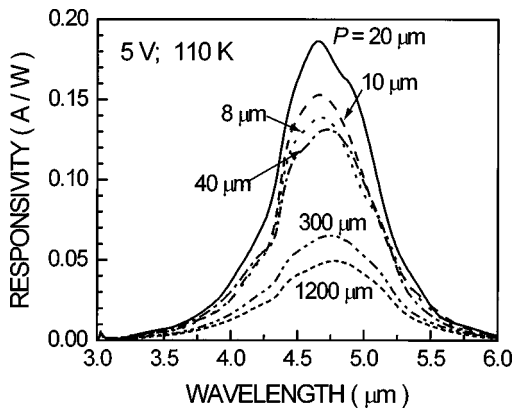[b)]Also with: U.S. Army Research Laboratory, 2800 Powder Mill Rd., Adelphi, MD 20783.

Appl. Phys. Lett., Vol. 75, No. 20, 15 November 1999

Chen *et al.*    3211



FIG. 2. The spectral responsivity of several C-QWIPs having $P = 8$, 10, 20, 40, 300, and 1200 $\mu$m, measured at 110 K and 5 V applied bias.

for an unpolarized incident light, where $t$ is the etching depth, $x$ is the distance away from the sidewalls, and $R_0$ is a constant. The double integral in Eq. (2) is for cross sectional integration of the optical intensity. $R_0$ accounts for the finite detector photoresponse not coming from the above-mentioned sidewall reflection, but also contributes as part of the quantum efficiency $\eta(P)$ in Eq. (2). $R_0$ may result from the presence of random surface scattering and the coupling of the $p$-polarized light by two of the mesa edges.[5] Its values can be obtained from the responsivity of a large area detector without corrugations. As a function of $P$, $R$ is expected to first increase with $P$, due to the increase of light-absorbing material within a corrugation unit. However, as $P$ becomes larger than $1/\alpha$, the material at the center of a corrugation unit receives little reflected light, while the total number of reflecting sidewalls is reduced. $R$ then decreases. The functional form of $R$ is therefore determined by $\alpha$. The remaining prefactor $g$ in Eq. (2) accounts for the overall magnitude of $R$. By fitting $R$ as a function of $P$, the values of $\alpha$, $g$, and $R_0$ can be uniquely determined.

The sample we used for the illustration of this technique is a mid-wavelength (MW) bound-to-quasibound QWIP, designed to peak at 4.3 $\mu$m. The active material consists of 20 periods of 300 Å $Al_{0.4}Ga_{0.6}As$ barriers and 5 Å GaAs/25 Å $In_{0.28}Ga_{0.72}As$/5 Å GaAs wells. The doping density in the InGaAs layer is $2.0 \times 10^{18}$ cm$^{-3}$. The total active material thickness is 7000 Å. On top of this material, a thick (1.8 $\mu$m) $n^+$ GaAs layer is grown as the contact layer. With this thick
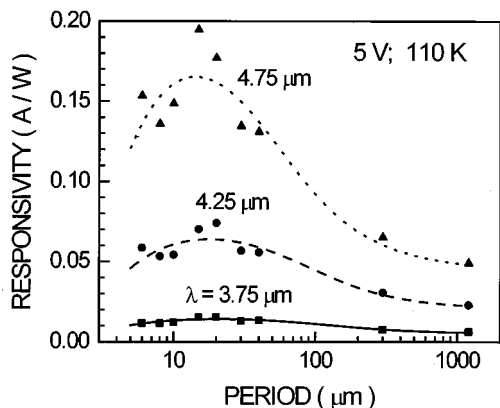


FIG. 3. The responsivity as functions of $P$ at three wavelengths $\lambda = 3.75$ $\mu$m (squares), 4.25 $\mu$m (circles), 4.75 $\mu$m (triangles), and their fits using Eq. (2).
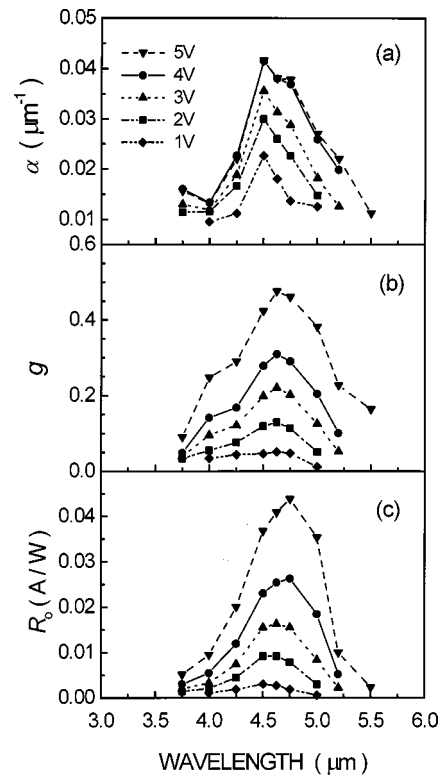


FIG. 4. (a) The absorption coefficient $\alpha$, (b) the photoconductive gain $g$, and (c) the responsivity $R_0$ as functions of wavelength, deduced from the curve fitting at different biases.

contact layer, a total depth of $t = 2.8$ $\mu$m has to be etched to expose the active volume. Since part of the reflected light is traveling in the nonabsorbing contact layer, the resultant $\alpha$ is the average absorption coefficient of an inhomogeneous medium (quantum wells plus contact layer), and is therefore smaller than if the entire volume were filled with the active material. The smaller $\alpha$ gives a smaller $\eta$ in Eq. (2). As a result, with a thin active QW region, the quantum efficiency of this MW QWIP is expected to be small. Its value will increase as we include more QW periods in the device.

In the experiment, a batch of nine C-QWIP samples, with period $P$ varying from 6 to 1200 $\mu$m, were prepared. Although these devices have been characterized at various temperatures to reveal the temperature dependence, we report here only the results obtained at $T = 110$ K, the background limited temperature for most C-QWIPs we prepared. A full report on the temperature dependence and the results for samples with other absorption wavelengths will be given in the near future.

The spectral responsivity $R$ of each C-QWIP was measured, using the ac lock-in technique, at several substrate biases V. At $V = 1$ V, the responsivity of the detectors is peaked at wavelength $\lambda_p = 4.5$ $\mu$m. As bias increases, $\lambda_p$ gradually shifts to longer wavelengths. At $V = 5$ V, $\lambda_p$ is equal to 4.75 $\mu$m, as illustrated in Fig. 2 for several representative C-QWIPs. It is clear from Fig. 2 that $R$ indeed depends on $P$. We also note that for each C-QWIP $R$ increases rapidly with V. For example, the peak responsivity for the C-QWIP with $P = 20$ $\mu$m increases from 11 to 186 mA/W as V increases from 1 to 5 V. In the past, this increase in $R$ was generally attributed to the increase of $g$.

With the information of $R$ for different $P$, curves of $R$ vs

$P$ can be plotted at different $\lambda$ and V. Illustrated in Fig. 3 are the representative results at 5 V, for three particular wavelengths 3.75, 4.25, and 4.75 $\mu$m. Note that the largest $R$ is obtained at $P=15$ $\mu$m. For each wavelength, a curve fitting with $\alpha$, $g$, and $R_0$ as free parameters is performed using Eq. (2). The result of fitting is also shown in Fig. 3. For each curve, only one unique set of parameters gives the best fit. Despite some scatter in the data, the model is still able to describe the general trend that $R$ first increases with increasing $P$, and then decreases at large $P$. Since the deviation of the data from the fitted curves is independent of $\lambda$, the scatter is most likely due to the processing nonuniformity.

The three parameters $\alpha$, $g$, and $R_0$, deduced at various V and $\lambda$, are shown in Figs. 4(a), 4(b), and 4(c), respectively. Contrary to the redshift of $R$, the peak wavelength for $\alpha$ is always located at 4.5 $\mu$m for all biases, indicating a negligible Stark shift in this material. The increasing magnitude of $\alpha$ with bias was, however, not expected in the past. Nevertheless, it is consistent with a report[6] that $R$ of a MW detector can increase by a factor of 2 between $T=125$ and 150 K. We attribute both phenomena to the ionization of deep-level donors in the barrier region under respective conditions. In the present case, the transfer of electrons from the donors to the QWs under field ionization increases $\alpha$ under bias.

It is clear from Fig. 4(b) that the photoconductive gain $g$ has strong bias dependence. The relatively uniform $g$ at low biases develops into a large peak at 4.7 $\mu$m at large biases. The fact that $g$ is peaked at around 4.7 $\mu$m (corresponding to a final state energy of 297 meV) is a result of two competing factors. At short wavelengths, the initiation of intervalley scattering into the $X$ and $L$ valleys in the barriers (both located at 320 meV for Al molar ratio of 0.4) reduces the electron mobility, and hence decreases the gain. At long wavelengths, on the other hand, the smaller carrier lifetime and the smaller tunneling probability, both implicitly included in $g$, make the value of $g$ small. Depending on the material structure and the bias applied to the detector, the value of $g$ can vary substantially across the excitation spectrum. This analysis clearly indicates that, in this MW sample, the redshift in $R$ results from the change of $g$. For other QWIP structures in which the electron levels are more sensitive to the bias, the result may be different.

From the results of the fitting, we also have a better understanding of the bias dependence of $R$. For the detector with $P=20$ $\mu$m, the peak responsivity increases 16 times from $V=1$ V to V$=5$ V, which can be resolved into the twofold increase in $\alpha$ [Fig. 4(a)] and the eightfold increase in

$g$ [Fig. 4(b)]. The fact that the peak wavelengths for $\alpha$ and $g$ are different explains the appearance of a shoulder in $R$ at 4.5 $\mu$m besides its main peak at 4.75 $\mu$m shown in Fig. 2.

In comparison, we also measured the noise of the 300 K background photocurrent $I_p$. The noise gain $g_n$, which was then deduced from the expression $S_n=4eg_nI_p$ with $S_n$ being the noise power density, was 0.17 at 5 V. Although this value is close to the average photoconductive gain 0.25 in Fig. 4(b), it is far less than the peak value 0.5 at $\lambda=4.75$ $\mu$m. This difference can be explained by the following argument. At 300 K, the background photon flux rises rapidly with wavelength in the MW band, creating more low energy excitations. As a result, the background photocurrent is dominated by low energy photoelectrons. Since $g$ is a strong function of energy, the low energy average can be quite different from the peak value. If $g_n=0.17$, instead of the peak value 0.5 used to evaluate the peak quantum efficiency, the deduced $\eta$ would be larger by a factor of 3. Also note that when $g$ and $g_n$ are different, the 300 K background limited detectivity is no longer independent of $g$. Instead, it is proportional to $\sqrt{(g/g_n)}$. Substituting the fitted parameters into Eq. (2), we find that at 5 V, $\eta$(peak)$=9.3\%$ for $P=15$ $\mu$m. The corresponding absorption length is 25 $\mu$m. We did not take into account the light interference effect in this work.

Figure 4(c) shows the value of $R_0$. It accounts for 27% of the total responsivity for $P=6$ $\mu$m. This percentage is consistent with our previous polarization measurement that the $p$ polarization of the incident light contributes 23% to the total signal.[5]

In conclusion, we have developed a simple yet powerful characterization technique for QWIPs. It allows direct, detailed, and accurate measurements on the intrinsic parameters $\alpha$ and $g$. The technique also gives more realistic information on the actual detector performance.

[1] D. A. Fulghum, Aviat. Week Space Technol., Feb. 3, p. 30 (1997).
[2] H. Kaplan, Photonics Spectra, June, p. 104 (1999).
[3] C. J. Chen, K. K. Choi, W. H. Chang, and D. C. Tsui, Appl. Phys. Lett. **71**, 3045 (1997).
[4] C. J. Chen, K. K. Choi, W. H. Chang, and D. C. Tsui, Appl. Phys. Lett. **72**, 7 (1998).
[5] C. J. Chen, K. K. Choi, L. Rohkinson, W. H. Chang, and D. C. Tsui, Appl. Phys. Lett. **74**, 862 (1999).
[6] A. C. Goldberg, J. W. Little, S. W. Kennerly, D. W. Beekman, and R. P. Leavitt, *Proceedings of the 6th International Workshop on Long Wavelength Infrared Detectors and Arrays*, edited by Li, Liu, Tidrow, and Gunapala (The Electrochemical Society, Pennington, NJ, 1998), Vol. 98-21, pp. 122–133.